EPJ Web of Conferences **96**, 01007 (2015)
DOI: 10.1051/epjconf/20159601007

Experiments with low-energy antimatter

G. Consolati [1, 2, a], S. Aghion [1, 2], C. Amsler [3], A. Ariga [3], T. Ariga [3], A. Belov [4], G. Bonomi [5, 6], P. Bräunig [7], J. Bremer [8], R.S. Brusa [9, 10], L. Cabaret [11], M. Caccia [12, 2], R. Caravita [13, 14], F. Castelli [15, 2], G. Cerchiari [16], K. Chlouba [17], S. Cialdi [15,2], D. Comparat [11], A. Demetrio [7], H. Derking [8], L. Di Noto [13, 14], M. Doser [8], A. Dudarev [8], A. Ereditato [3], R. Ferragut [1, 2], A. Fontana [6], S. Gerber [8], M. Giammarchi [2], A. Gligorova [18], S. Gninenko [4], S. Haider [8], S. Hogan [19], H. Holmestad [20], T. Huse [20], E. J. Jordan [16], J. Kawada [3], A. Kellerbauer [16], M. Kimura [3], D. Krasnicky [13, 14], V. Lagomarsino [13, 14], S. Lehner [21], C. Malbrunot [8, 21], S. Mariazzi [21], V. Matveev [4], Z. Mazzotta [15, 2], G. Nebbia [22], P. Nedelec [23], M. Oberthaler[7], N. Pacifico [18], L. Penasa [9, 10], V. Petracek [17], C. Pistillo [3], F. Prelz [2], M. Prevedelli [24], L. Ravelli [9, 10], C. Riccardi [25, 6], O.M. Røhne [20], S. Rosenberger [8], A. Rotondi [25, 6], M. Sacerdoti [15, 2], H. Sandaker [20], R. Santoro [12, 2], P. Scampoli [3, 26], M. Simon[21], M. Spacek [17], J. Storey [3], I. M. Strojek [17], M. Subieta [5, 6], G. Testera [14], E. Widmann [21], P. Yzombard [11], S. Zavatarelli [14] and J. Zmeskal [21]

[1] Politecnico of Milano, Piazza Leonardo da Vinci 32, 20133 Milano, Italy
[2] INFN Milano, via Celoria 16, 20133 Milano, Italy
[3] Laboratory for High Energy Physics, Albert Einstein Center for Fundamental Physics, University of Bern, 3012 Bern, Switzerland
[4] Institute for Nuclear Research of the Russian Academy of Science, Moscow 117312, Russia
[5] Department of Mechanical and Industrial Engineering, University of Brescia, via Branze 38, 25123 Brescia, Italy
[6] INFN Pavia, via Bassi 6, 27100 Pavia, Italy
[7] Kirchhoff-Institute for Physics, Heidelberg University, Im Neuenheimer Feld 227, 69120 Heidelberg, Germany
[8] Physics Department, CERN, 1211 Geneva 23, Switzerland
[9] Department of Physics, University of Trento, via Sommarive 14, 38123 Povo, Trento, Italy
[10] TIFPA/INFN Trento, via Sommarive 14, 38123 Povo, Trento, Italy
[11] Laboratory Aimé Cotton, CNRS, University of Paris-Sud, ENS Cachan, Bât. 505, 91405 Orsay, France
[12] Department of Science, University of Insubria, Via Valleggio 11, 22100 Como, Italy
[13] Department of Physics, University of Genova, via Dodecaneso 33, 16146 Genova, Italy
[14] INFN Genova, via Dodecaneso 33, 16146 Genova, Italy
[15] Department of Physics, University of Milano, via Celoria 16, 20133 Milano, Italy
[16] Max Planck Institute for Nuclear Physics, Saupfercheckweg 1, 69117 Heidelberg, Germany
[17] Czech Technical University, Prague, Brehová 7, 11519 Prague 1, Czech Republic
[18] Institute of Physics and Technology, University of Bergen, Allégaten 55, 5007 Bergen, Norway
[19] University College London, Gower Street, London WC1E 6BT, United Kingdom
[20] Department of Physics, University of Oslo, Sem Sælandsvei 24, 0371 Oslo, Norway
[21] Stefan Meyer Institute for Subatomic Physics, Austrian Academy of Sciences, Boltzmanngasse 3, 1090 Vienna, Austria
[22] INFN Padova, via Marzolo 8, 35131 Padova, Italy
[23] Institute of Nuclear Physics, CNRS/IN2p3, University of Lyon 1, 69622 Villeurbanne, France
[24] University of Bologna, Viale Berti Pichat 6/2, 40126 Bologna, Italy
[25] Department of Physics, University of Pavia, via Bassi 6, 27100 Pavia, Italy
[26] Department of Physics, University of Napoli Federico II, Complesso Universitario di Monte S. Angelo, 80126, Napoli, Italy

Abstract. Investigations on antimatter allow us to shed light on fundamental issues of contemporary physics. The only antiatom presently available, antihydrogen, is produced making use of the Antiproton Decelerator (AD) facility at CERN. International collaborations currently on the floor (ALPHA, ASACUSA and ATRAP) have succeeded in producing antihydrogen and are now involved in its confinement and manipulation. The AEGIS experiment is currently completing the commissioning of the apparatus which will generate and manipulate antiatoms. The present paper, after a report on the main results achieved with antihydrogen physics, gives an overview of the AEGIS experiment, describes its current status and discusses its first target.

[a]Corresponding author: giovanni.consolati@polimi.it

1. Introduction

Antimatter is a hot topic in contemporary physics, owing to its important role in our understanding of fundamental interactions. Precision spectroscopy measurements on antimatter are considered an important test of the validity of the CPT theorem [1]. In fact, a possible violation of the theorem is envisaged in some extensions of the Standard Model [2]. Another issue concerns the gravitational interaction on antimatter. The weak equivalence principle (WEP) postulates that the trajectory and the velocity of a body falling in an external gravitational field is not affected by its composition, but depends only on its initial position and velocity. Many careful tests verified the WEP at 10^{-13} level for ordinary matter [3]. Measurements with charged antimatter are very complicated, owing to the overwhelming effect of residual electromagnetic forces [4]. Indirect arguments have been raised against a different acceleration of antimatter with respect to matter; however, some attempts to formulate quantum theories of gravity, or to unify gravity with the other forces [5] consider the possibility of a non-identical gravitational interaction between matter and antimatter, which could even repel each other, in spite of being self-attractive [6]. A possible gravitational repulsion between matter and antimatter could be consistent with the standard formulation of general relativity and would not imply any modification of the theory [7].

Therefore, neutral antimatter, that is, antiatoms, are of great interest to investigate the gravitational interaction. The only antiatom which will be possible to investigate in the next future is antihydrogen, $\bar{H}$. In particular, a measurement of the gravitational acceleration $\bar{g}$ on $\bar{H}$, even with a few percent precision, would be scientifically relevant, as it would represent the first direct measurement of the gravitational interaction between matter and antimatter.

The first production of $\bar{H}$ occurred in 1995 at CERN [8] and two years later at Fermilab [9]; confinement of antihydrogen was however impossible, the energies being of the order of a few GeV. The ATHENA [10] and the ATRAP [11] experiments in 2002 obtained for the first time $\bar{H}$ with low kinetic energy (actually, around 1 meV, corresponding to a temperature of about ten K). Nowadays, four experiments (ALPHA, ASACUSA, ATRAP and AEGIS) are currently running at CERN, with the aim to produce antihydrogen with more advanced features (*e.g.* cold $\bar{H}$ for spectroscopy studies), by using the (AD) facility, which supplies about 10^7 antiprotons ($\bar{p}$) - with kinetic energy of 5.3 MeV – in the form of pulses of about 200 ns and at a repetition rate of 100 s. Since 2014 another experiment, BASE, is also on the floor for precise measurements on $\bar{p}$.

The ALPHA, ASACUSA and ATRAP collaborations produce antihydrogen by means of the following three-body reaction:

$$e^+ + e^+ + \bar{p} \rightarrow \bar{H} + e^+ \qquad (1)$$

Positrons and $\bar{p}$ are first confined into electromagnetic nested Penning traps [12], then they are mixed, so that the reaction (1) takes place. In ALPHA intense magnetic fields (about 3 T) and pulsed electric fields assure both the radial and axial confinement of $\bar{p}$, which are cooled through sympathetic scattering with low energy electrons inserted into the trap. Positrons are guided by means of electric fields in the Penning trap, where they are manipulated to reach the suitable energy and density to interact with antiprotons and produce antihydrogen. $\bar{H}$ confinement is achieved by means of a radial magnetic multipole trap which is superimposed on the axial magnetic solenoid field for plasma confinement. In 2011 ALPHA reported the longest achieved $\bar{H}$ confinement, 1000 s, together with the first measurement of the energy distribution of the trapped antiatoms [13]; this result was obtained by means of an octupolar non-homogeneous magnetic field. Two years later ALPHA attempted a first gravitational test on neutral trapped antimatter. $\bar{H}$ atoms in a trap were released and the up-down asymmetry of the annihilations was measured allowing the collaboration to find a constraint (at 95% confidence level) of $-65 < M_g/M_i < 110$ for the ratio between the gravitational and the inertial mass of $\bar{H}$ [14].

The ATRAP collaboration has previously generated $\bar{H}$ through the interaction of $\bar{p}$ (collected in a Penning trap) with positronium (Ps) [15]. This is produced by means of Cs atoms in Rydberg state (that is, highly excited atoms) which interact with positrons accumulated in a second Penning trap. The whole process can be described by the following charge exchange reactions:

$$Cs^* + e^+ \rightarrow Ps^* + Cs^+ \qquad (2a)$$
$$Ps^* + \bar{p} \rightarrow \bar{H} + e^- \qquad (2b)$$

Although the cross section of the entire process (2) is lower than that of reaction (1), antihydrogen is produced with lower energy, therefore, it can be trapped more easily.

In 2013 ATRAP published the most precise measurement to date of the antiproton magnetic moment $\mu_{\bar{p}}$ [16]. $\bar{p}$ were captured in a Penning trap in the presence of a magnetic field of about 5 T and their spin flip and cyclotron frequencies, f_s and f_c, respectively, were measured. From their ratio the antiproton $g_{\bar{p}}$ factor was obtained: $f_s/f_c = g_{\bar{p}}$. It resulted $\mu_{\bar{p}} = \mu_p$ within 5 ppm, consistent with the predictions of the CPT theorem.

Precise measurement of the antiproton magnetic moment is also a goal of the BASE collaboration. They recently reported the direct measurement of the magnetic moment of a single proton [17] using the double Penning trap technique [18], with improvement of the precision by a factor of about 760 with respect to the previous measurement [19]. Since the same method can be applied also to antiprotons, BASE is working at the AD of CERN to obtain the magnetic moment of the antiproton with a precision at ppb level, which would provide one of the most sensitive tests of CPT symmetry.

The ASACUSA collaboration proposed the cusp trap [20] as an alternative to the standard method to produce $\bar{H}$ in Penning traps. In the cusp trap positrons and

antiprotons are trapped in a nested Penning trap located in the spindle cusp region at the maximum magnetic field point [21]. The inhomogeneous cusp field in the center is then used to polarize neutral antihydrogen atoms leaving the formation region. In this way cold $\bar{H}$ (a few K) has been produced [22] which can be transported outside the trap. By using this technique a continuous beam of $\bar{H}$ atoms has been recently obtained [23]. In 2011 ASACUSA carried out laser spectroscopy on antiprotonic helium ($\bar{p}He^+$) [24] which allowed them to obtain the value of the antiproton-to-electron mass ratio with a precision of less of 2 ppb.

2. Overview of the AEGIS experiment

The AEGIS collaboration (Antimatter Experiment: Gravity, Interferometry, Spectroscopy) began in 2007 in order to study fundamental physics with antimatter systems. The primary aim is to measure the gravitational acceleration $\bar{g}$ on $\bar{H}$. In the first stage of the AEGIS experiment the goal is to produce $\bar{H}$ with energy below 1 K and to measure its free fall in the Earth's gravitational field, with a precision of 1%. Later on, depending on the availability of sufficiently cold $\bar{H}$, it will become possible to carry out tests on the CPT theorem by spectroscopic methods.

As far as the gravity measurement is concerned, a beam of cold $\bar{H}$ will be formed and its vertical fall through a moiré deflectometer will be registered. The essential steps to produce cold $\bar{H}$, as well as to measure its gravitational acceleration can be summarized under the following items: a) capture and accumulation of antiprotons coming from the AD facility at CERN in a Penning-Malmberg trap; b) $\bar{p}$ cooling to sub-K temperatures; c) production of positrons and their storage into an accumulator; d) production and emission into vacuum of cold (< 150 K) Ps formed from impinging a positron bunch on a suitable nanoporous target; e) Ps excitation in a Rydberg state (Ps*) by means of suitable laser pulses; f) formation of cold Rydberg $\bar{H}$ ($\overline{H^*}$) from a charge exchange reaction between antiprotons and Ps^*; g) extraction of $\overline{H^*}$ atoms by means of inhomogeneous electric fields (Stark acceleration technique); h) measurement of their vertical deflection due to gravitational acceleration using a moiré deflectometer coupled to a position sensitive detector.

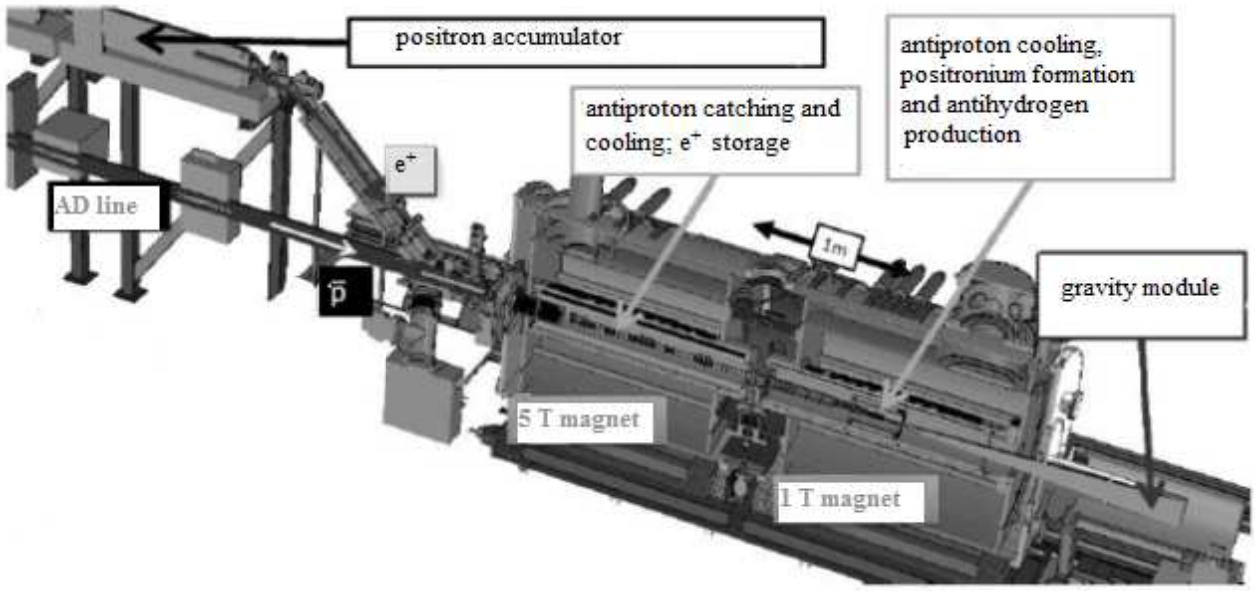

Figure 1 – Schematic drawing of the main components of the AEGIS apparatus (reprinted figure from ref. 41. Copyright (2013) by AIP Publishing LLC. DOI: 10.1063/1.4796070).

The core of the AEGIS apparatus consists of the positron system and a cryogenic system in ultra high vacuum composed by two magnets (5 T and 1T), where a complex system of traps is located (Figure 1). Antiprotons delivered from the AD pass through a degrader (a stack of Al foils, with variable thicknesses) and are caught in a trap placed in the 5 T magnet. Preloaded electrons provide electron cooling of $\bar{p}$. Then, $\bar{p}$ are transferred into the 1 T region for further cooling, taking advantage of a dilution refrigerator (to be installed) as well as a resistive active-feedback cooling system. The possibility of sympathetic cooling with La anions is also under study. The final design envisages a cloud of 10^5 $\bar{p}$ at equivalent temperature below 1 K; this temperature is an important factor influencing the final energy of $\bar{H}$.

Positrons generated by a ^{22}Na source (activity ≈ 740 MBq) are slowed down by means of a solid Ne moderator and captured in a Surko-type [25] trap. Afterwards, they are dumped onto an accumulator, able to stack up to 10^8 positrons in 200 s. Then, positrons are magnetically guided to the 1 T region where they impinge on a porous target. Pores are essential to cool positronium (Ps) through collisions with the pore walls. Eventually, a

fraction of Ps formed is re-emitted into vacuum at low energies (corresponding to a temperature < 150 K). Ps atoms interacting with the $\bar{p}$ cloud will produce $\bar{H}$ according to the charge exchange reaction (2b) (see figure 2).

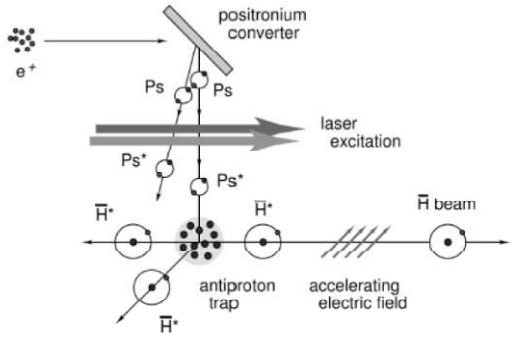

Figure 2 – Sketch of $\bar{H}$ production in AEGIS (reprinted figure from ref. 42. Copyright (2008) by Elsevier B.V. Doi:10.1016/j.nimb.2007.12.010).

Since the cross section of reaction (2b) increases with n^4, where n is the principal quantum number of Ps, it is important to produce Ps in a Rydberg state. This will occur by means of two laser excitations of Ps emitted from the porous target: a first UV laser (at 205 nm) will bring Ps from the ground to the $n = 3$ state; a second laser pulse (tunable in the range 1650-1700 nm) will excite Ps to the final Rydberg state [26].

As a consequence of the reaction (2b) $\bar{H}$ will be formed in a Rydberg state, hence, with a large electric dipole moment; this allows one to accelerate the antiatom in the presence of an inhomogeneous electric field. In this way, $\bar{H}$ will reach a velocity around 500 m/s; this technique, already tested with hydrogen [27], will allow the antiatoms to be driven along the gravity measurement module. Their time of flight T ($\approx 10^{-3}$ s, three orders of magnitude higher than the formation time) will be measured from the time span between the Stark acceleration time and a timing detector at the end of the gravity module. The latter (moiré deflectometer) consists of two identical gratings, normal to the trajectory of $\bar{H}$, having (in the original plan) periodicity 40 μm, transmittance 30% and placed at a distance L = 50 cm from each other [28]. In the final, optimized design the above figures could slightly change. Among the particles traversing the two gratings only those ones having well defined trajectories are selected (figure 3) and produce a fringe pattern in a third plane, located at the same distance L from the second grating. Such a pattern is shifted in the presence of a force; in the case of (anti)gravity the shift δ depends on both T and $\bar{g}$: $\delta = -\bar{g}T^2$. Therefore, $\bar{g}$ can be obtained by fitting the shift versus the time of flight on an event-by-event basis. The data will be obtained by means of a hybrid detector placed in the third plane. The detector is formed (figure 4) by a thin foil of silicon, where annihilation events will take place and which separates the UHV region from the region containing a stack of nuclear emulsion films (for the measurement of δ), in ordinary vacuum. Behind the emulsions are two planes of scintillating fibers; both the fibers and the silicon foil will measure the time of flight T of each annihilation event.

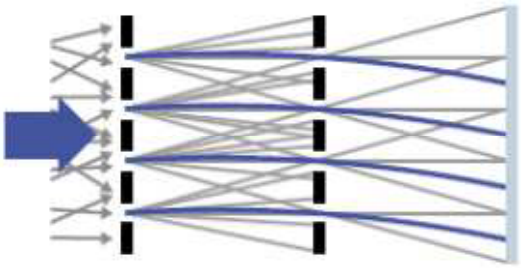

Figure 3 – The moiré deflectometer. The trajectories of undisturbed particles (grey lines) are modified by the presence of a force (blue lines) and a shift of the fringe pattern occurs (reprinted figure from ref. 37. Copyright (2014) by Macmillan Publishers Limited. DOI: 10.1038/ncomms5538).

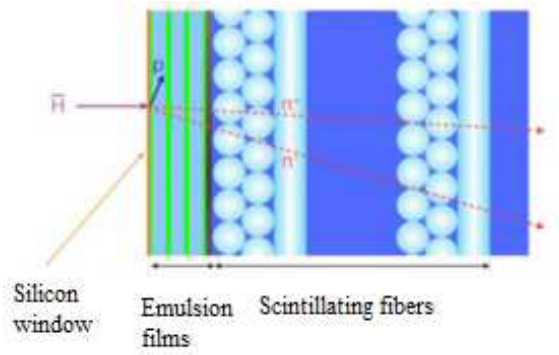

Figure 4 – The hybrid detector for measuring $\bar{H}$ annihilations (reprinted figure from ref. 40. Copyright (2014) by IOP Publishing Ltd. Doi:10.1088/1748-0221/9/01/C01061).

The production of $\bar{H}$ atoms and the formation of an antihydrogen beam are critical issues, which require a careful diagnostic system. For this purpose, a detector has been designed, working in challenging conditions; indeed, it must operate at 4 K, inside a 1 T magnetic field, in vacuum conditions (10^{-6} mbar) within a cylindrical volume surrounding the region of $\bar{H}$ formation. The power dissipation should be as low as possible (< 10 W) not to perturb the cryogenic environment. Last but not least, the detector must be fast enough to identify annihilations occurring during the time interval (1 ms) of pulsed $\bar{H}$ production. Such a Fast Annihilation Cryogenic Detector (FACT) [29] consists of four layers of 1 mm diameter multi-clad scintillating fibers coupled to clear fibers which have the task of transferring the optical signal from the cryogenic region onto an array of multi-pixel-photon-counters. Reconstruction of the position of the annihilation vertex along the axis of the antihydrogen beam will allow us to estimate the temperature of the beam. A resolution of 2.1 mm is expected.

3. Antihydrogen production procedure

Catching of the $\bar{p}$ coming from AD requires a suitable system of traps, which were designed by members of the AEGIS collaboration. A Penning-Malmberg trap is

located in a cold bore (7 K) of the 5 T magnet. Up to 90% of the caught $\bar{p}$ (around 10^5 per one AD shot) are cooled to eV energies within 40 s by about 10^9 preloaded electrons, located in a small potential well. Trapping of cold $\bar{p}$ up to 600 s was measured, limited by the temperature in the cryogenic system. Improvement of the confinement time up to a factor four is expected in the future.

A more complex trap system, formed by four Penning-Malmberg traps, is located in the 1 T magnet. The first trap compresses the particles coming from the 5 T magnet by means of a rotating wall electrodes system [30]. Then, two traps follow: an on-axis trap transfers $\bar{p}$ into the $\bar{H}$ production trap, where $\bar{p}$ cooling to the final temperatures takes place. Positrons are moved off-axis into a further trap by using the excitation of the diocotron mode of the positron plasma [31]. In this trap high voltage electrodes accelerate positrons onto the target where Ps formation occurs.

Concerning positrons, we are able to store up to $8 \cdot 10^7$ particles in 500 s within the accumulator. Transfer of the particles in the 5 T magnet occurs with high efficiency; we do not observe losses when the positron beam is compressed to 2.2 mm (FWHM). After the commissioning phase a new radioactive source of 1.8 GBq will be installed, which will further increase the number of positrons available in the future.

Several studies on Ps production were carried out in the past years; porous targets showed promising results. In particular, mesoporous silicon chips [32] by electrochemical etching of a Si p-type (100) were obtained with tunable mesopore sizes in the range 5-20 nm. High Ps formation and emission in vacuum was demonstrated, with the presence of a thermal fraction in the sample temperature range 150-300 K [33]. Powders of swelled-MCM-41 type material in pellet form [34] and silica aerogel of very high porosity [35] were also studied in vacuum, in a temperature range between 8 and 293 K. Also in these materials high Ps formation was observed, which does not depend on the temperature of the sample. The presence of hydrophobic patches on the porous structure of aerogel and MCM-41 [36] hinders water absorption and condensation at low temperatures. To complete Ps studies a vacuum chamber has been installed at the output of the positron accumulator, to be used when the positron beam is not requested by the AEGIS apparatus (*e.g.* when $\bar{p}$ are not available from AD), to measure the Ps conversion efficiency of the different porous materials at cryogenic temperatures. It will be also useful to carry out Ps spectroscopy, in order to set the best parameters of the laser system.

Ps excitation to Rydberg states will be obtained by a two-step process. The laser system is composed by two subsystems: one for the generation of UV radiation, the other one in the IR range [26]. A 6 ns Q-switched Nd:YAG laser produces radiation at 1064 nm. This passes through a second harmonic crystal to double the frequency; the energy of each pulse is about 75 mJ. A beam splitter sends a small part of the 532 nm pulse to a first optical parametric generator (OPG1) producing 894 nm radiation. The remaining energy at 532 nm is sent to a BBO non-linear crystal generating a second harmonic radiation at 266 nm. The two radiations, at 266 nm and 894 nm, are finally summed up to produce the UV radiation at 205 nm, necessary to bring Ps to $n = 3$. The second subsystem uses the same Nd:YAG laser, which feeds an OPG2-OPA (optical parametric amplifier) source, able to produce a tunable wavelength in the range 1650-1700 nm, pulse length < 10 ns and pulse energy up to 2 mJ. This second pulse will produce Rydberg Ps. Fine wavelength tuning is obtained by exploiting the temperature dependence of the wavelength at the output of the Periodically Poled Potassium Titanil Phosphate crystal, which forms the core of the OPG. A temperature controlled heater can change the temperature of the crystal between 25°C and 130°C. In this way a selection of the final Ps excited energy, from $n = 16$ up to the ionization limit, is possible. The whole laser system was assembled and tested at CERN and it is ready to operate.

The design of the moiré deflectometer will take advantage of the experience gained on a compact prototype device, working with antiprotons [37]. It is formed by two parallel gratings (distance 25 mm from each other) and an emulsion detector at a distance 25 mm from the second grating. A beam of particles passing through the deflectometer produces a fringe pattern on the detector, which is shifted in the presence of a force. To infer the force, a comparison with a near-field interference pattern produced by light is carried out. An additional transmission grating in direct contact with the emulsion is illuminated simultaneously with the moiré deflectometer, with antiprotons as well as with light. This provides a reference for alignment, since the pattern behind the contact grating cannot show any dependence on a force. The results showed a shift in the moiré pattern with respect to the interference pattern due to the light, which corresponds to a force acting on $\bar{p}$ of about 530 ± 50 aN (stat) ± 350 aN (syst). By identifying such a force with a Lorentz force due to a magnetic field, a magnetic induction $B \sim 7.4$ G was found, which is good agreement with the magnetic induction ~ 10 G measured at the position of the deflectometer and normal to the direction of $\bar{p}$. These results are essential for the final design of the deflectometer working with $\bar{H}$. Indeed, the $\bar{H}$ fringe pattern due to gravity is expected to be comparable to the one observed in the case of antiprotons. It is true that the gravitational force acting on $\bar{H}$ is ten orders of magnitude smaller than the sensitivity level reached with the prototype device, but the resolution of the setup will be improved by scaling up the deflectometer and the detector. Furthermore, the velocity of $\bar{H}$ should be four orders of magnitude smaller than the velocity of the $\bar{p}$ used in the experiment described above.

The $\bar{H}$ detector is in advanced phase of commissioning. A planar strip silicon detector has been tested to provide time of flight information and a position resolution of 7-8 μm. The thinness of the detector (50 μm) grants limited scattering of the annihilation products, to be detected by the subsequent emulsion films, and improves position resolution [38].

Emulsion films consist of AgBr crystals uniformly distributed in a gel where a latent track is formed as a

consequence of the transit of an ionizing particle. After development, the latent track becomes visible in an optical microscope. Fast automated scanning systems for the track analysis renewed interest in the application of emulsion films, overcoming the problem of the manual scanning procedure, which is very time consuming. Application to the AEGIS experiment is challenging, due to the severe experimental conditions (vacuum and low temperatures) for the emulsions. To cope with these problems a new kind of emulsion gel was developed, which can be used in vacuum. Measurements with a 100 keV antiproton beam showed successful reconstructions of the $\bar{p}$ annihilation events with a resolution of ~ 1 μm, by using the ionizing secondary tracks [39]. The attainable precision in the measurement of $\bar{g}$ is strongly related to the spatial resolution: to get $\bar{g}$ with 1% uncertainty less than 1000 events are required, with the given resolution [40]. For the sake of comparison, more than 10^4 events would be required with a spatial resolution of 10 μm. The influence of the temperature on the background and sensitivity of the emulsions are at present under investigation.

Concerning the FACT detector, tests of the scintillating fibers performed in a 4 K cryostat were carried out to investigate the effects of cryogenic temperatures on the light yield, decay time and lifetime of the fibers. Cosmic rays were exploited to test the detector. The results [29] show only a slight decrease (≈ 10%) of the rate of events detected by the fibers when passing from room temperature to 4 K. Furthermore, no mechanical damage resulted after many thermal cycles to 4 K.

4. Conclusion and outlook

Various experiments on cold antimatter are actually running, commissioning or are approved at CERN, with the aim to perform precision tests on fundamental physics. The AEGIS collaboration is concluding the construction of the apparatus planned to perform experiments on antihydrogen. In 2014 we carried out measurements with $\bar{p}$ as well as with positrons; we are currently analyzing the collected data in order to optimize the involved parameters. The challenge is to produce antiatoms by means of a charge exchange reaction, a new route able to supply an $\bar{H}$ beam with equivalent temperatures below 1 K. This will give possibility to test, for the first time, the weak equivalence principle on antimatter, at the 1% level.

Current experiments are limited by the trapping efficiency of antiprotons, coming from AD at 5.3 MeV, which have to be slowed down before being manipulated. In 2017 ELENA (Extra Low Energy Antiproton Ring), a further deceleration step, should start operation, lowering the energy of the available antiprotons to 100 keV. This will increase the $\bar{p}$ catching efficiency by up two orders of magnitude. Then, it will be possible to run several experiments in parallel (at present each experiment has a fraction of the beam time available), opening new perspectives in cold antimatter physics.

References

1. N. F. Ramsey, Physica Scripta **T59**, 323 (1995)
2. D. Colladay and V. A. Kostelecky, Phys. Rev. D **55**, 6760 (1997)
3. E. G. Adelberger *et al*., Prog. Part. Nucl. Physics **62**, 102 (2009)
4. T.W. Darling *et al*., Rev. Mod. Phys. **64**, 237 (1992)
5. J. Barrow and R. Scherrer, Phys. Rev. D **70,** 103515 (2004)
6. G. J. Ni, in: *Relativity, Gravitation, Cosmology*, edited by V. V. Dvoeglazov and A. A. Espinoza Garrido (Nova Science Publications), p. 123 (2004)
7. M. Villata, Europhys. Lett. **94**, 20001 (2011)
8. G. Baur *et al*., Phys. Lett. B **368**, 251 (1996)
9. G. Blanford *et al*., Phys. Rev. Lett. **80,** 3037 (1997)
10. M. Amoretti *et al*. (ATHENA collaboration), Nature **419**, 456 (2002)
11. G. Gabrielse *et al*. (ATRAP collaboration), Phys. Rev. Lett. **89**, 213401 (2002)
12. G. Gabrielse *et al*., Phys. Rev. Lett. **57**, 2504 (1986)
13. G. B. Andresen *et al*. (ALPHA collaboration), Nature Physics **7**, 558 (2011)
14. C. Amole *et al*., Nature Comm. **4**, 1785 (2013)
15. C. Storry *et al*. (ATRAP collaboration), Phys. Rev. Lett. **93**, 263401 (2004)
16. J. Di Sciacca *et al*. (ATRAP collaboration), Phys. Rev. Lett. **110**, 130801 (2013)
17. A. Mooser *et al*., Nature **509**, 596 (2014)
18. H. Häffner *et al*., Eur. Phys. J. D **22**, 163 (2003)
19. J. Di Sciacca and G. Gabrielse, Phys. Rev. Lett. **108**, 153001 (2012)
20. A. Mohri and T. Yamazaki, Europhys. Lett. **63**, 207 (2003)
21. H. Saitoh, A. Mohri, Y. Enomoto, Y. Kanai and Y. Yamazaki, Phys. Rev. A **77**, 051403 (2008)
22. Y. Enomoto *et al*. (ASACUSA collaboration), Phys. Rev. Lett. **105**, 243401 (2010)
23. N. Kuroda *et al*. (ASACUSA collaboration), Nature Comm. **5**, 3089 (2014)
24. M. Hori *et al*. (ASACUSA collaboration), Nature **475**, 484 (2011)
25. R. G. Greaves and C.M. Surko, Phys. Plasmas **4**, 1528 (1997)
26. S. Cialdi *et al*., Nucl. Instr. & Methods B **269**, 1527 (2011)
27. E. Vliegen, S. D. Hogan, H. Schmutz, and F. Merkt, Phys. Rev. A **76**, 023405 (2007)
28. M. K. Oberthaler, S. Bennet, E. M. Rasel, J. Schniedmayer and A. Zeilinger, Phys. Rev. A **54**, 3165 (1996)
29. J. Storey *et al*. (AEGIS collaboration), Nucl. Instr. Meth. in Phys. Res. A **732**, 437 (2013)
30. D. H. E. Dubin and T. M. O'Neil, Rev. Mod. Phys. **71**, 87 (1999)
31. C. Canali *et al*., Eur. Phys. J. D **65**, 499 (2011)
32. S. Mariazzi, P. Bettotti, S. Larcheri, L. Toniutti and R. S. Brusa, Phys. Rev. B: Condens. Matter Mater. Phys. **81**, 235418 (2010)
33. S. Mariazzi, P. Bettotti and R. S. Brusa, Phys. Rev. Lett.**104**, 243401 (2010)

34. G. Consolati, R. Ferragut, A. Galarneau, F. Di Renzo and F. Quasso, Chem. Soc. Rev. **42**, 3821 (2013)
35. R. Ferragut *et al.* J. Phys. Chem. C **117**, 26703 (2013)
36. M. F. Ottaviani, A. Galarneau, D. Desplantier-Giscard, F. Di Renzo and F. Fajula, Microporous Mesoporous Mater. **44–45**, 1 (2001)
37. S. Aghion *et al.* (AEGIS collaboration), Nature Comm. **5**, 4538 (2014)
38. N. Pacifico *et al*. (AEGIS collaboration), Nucl Instr. Meth. in Phys. Res. A, **765**, 161 (2014)
39. M. Kimura *et al*. (AEGIS collaboration), Nuclear Instr. Meth. in Phys Res A **732**, 325, (2013)
40. M. Scampoli *et al*. (AEGIS collaboration), JInst **9**, C01061 (2014)
41. D. Krasnicky *et al*. (AEGIS collaboration), AIP Conf. Proc. **1521**, 144 (2013)
42. A. Kellerbauer *et al*. (AEGIS collaboration), Nucl. Instr. Meth. in Phys. Res. B **266**, 351 (2008)